Journal of Controlled Release 214 (2015) 12–22

Contents lists available at ScienceDirect

Journal of Controlled Release

journal homepage: www.elsevier.com/locate/jconrel

A liquid crystal of ascorbyl palmitate, used as vaccine platform, provides sustained release of antigen and has intrinsic pro-inflammatory and adjuvant activities which are dependent on MyD88 adaptor protein

María F. Sánchez Vallecillo [a], María M. Minguito de la Escalera [d], María V. Aguirre [a], Gabriela V. Ullio Gamboa [b], Santiago D. Palma [b], Leticia González-Cintado [d], Ana L. Chiodetti [a], Germán Soldano [c], Gabriel Morón [a], Daniel A. Allemandi [b], Carlos Ardavín [d,1], María C. Pistoresi-Palencia [a,1], Belkys A. Maletto [a,*]

[a] Departamento de Bioquímica Clínica, CIBICI (CONICET), Facultad de Ciencias Químicas, Universidad Nacional de Córdoba, Haya de la Torre y Medina Allende, Ciudad Universitaria, X5000HUA Córdoba, Argentina
[b] Departamento de Farmacia, UNITEFA (CONICET), Facultad de Ciencias Químicas, Universidad Nacional de Córdoba, Haya de la Torre y Medina Allende, Ciudad Universitaria, X5000HUA Córdoba, Argentina
[c] Departamento de Matemática y Física, INFIQC (CONICET), Facultad de Ciencias Químicas, Universidad Nacional de Córdoba, Haya de la Torre y Medina Allende, Ciudad Universitaria, X5000HUA Córdoba, Argentina
[d] Departamento de Inmunología y Oncología, CNB (CSIC), Darwin 3, 28049 Madrid, Spain

ARTICLE INFO

Article history:
Received 21 January 2015
Received in revised form 25 June 2015
Accepted 2 July 2015
Available online 15 July 2015

Keywords:
Liquid crystal
Ascorbyl palmitate
Nanostructure
Controlled release
Vaccine adjuvant
Danger-associated molecular patterns (DAMPs)

ABSTRACT

Modern subunit vaccines require the development of new adjuvant strategies. Recently, we showed that CpG-ODN formulated with a liquid crystal nanostructure formed by self-assembly of 6-O-ascorbyl palmitate (Coa-ASC16) is an attractive system for promoting an antigen-specific immune response to weak antigens. Here, we showed that after subcutaneous injection of mice with near-infrared fluorescent dye-labeled OVA antigen formulated with Coa-ASC16, the dye-OVA was retained at the injection site for a longer period than when soluble dye-OVA was administered. Coa-ASC16 alone elicited a local inflammation, but how this material triggers this response has not been described yet. Although it is known that some materials used as a platform are not immunologically inert, very few studies have directly focused on this topic. In this study, we explored the underlying mechanisms concerning the interaction between Coa-ASC16 and the immune system and we found that the whole inflammatory response elicited by Coa-ASC16 (leukocyte recruitment and IL-1β, IL-6 and IL-12 production) was dependent on the MyD88 protein. TLR2, TLR4, TLR7 and NLRP3-inflammasome signaling were not required for induction of this inflammatory response. Coa-ASC16 induced local release of self-DNA, and in TLR9-deficient mice IL-6 production was absent. In addition, Coa-ASC16 revealed an intrinsic adjuvant activity which was affected by MyD88 and IL-6 absence. Taken together these results indicate that Coa-ASC16 used as a vaccine platform is effective due to the combination of the controlled release of antigen and its intrinsic pro-inflammatory activity. Understanding how Coa-ASC16 works might have significant implications for rational vaccine design.

1. Introduction

Coa-ASC16 (or coagel) is a liquid crystal nanostructure formed by self-assembly of 6-O-ascorbyl palmitate (ASC16). The coagel phase is composed of surfactant lamellae separated by interlayers of strongly bound water molecules (Fig. 1A–B). ASC16 in water at room temperature is insoluble, but on heating, its solubility increases and it turns into a transparent dispersion above the critical micelle temperature. On cooling, water dispersion of ASC16 forms a liquid crystal structure called Coa-ASC16, which possesses a lamellar structure that exhibits sharp X-ray diffraction patterns and optical birefringence [1,2]. In previous studies, we reported the physicochemical characterization of Coa-ASC16 [1]. As ASC16 contains a hydrophobic portion (alkyl chain) and a polar group (ascorbic acid), this material has amphiphilic properties which provide an ideal environment for the solubilization of hydrophobic and hydrophilic molecules with redox activity of vitamin C being maintained. Previously, we have described the whole phase diagram of ASC16 in water with an interesting feature of this system being the way the water molecules interact with assembled ASC16 molecules. The water in this system is in three different states. The first hydration layer is composed of about 11 water molecules per ASC16 molecule, which are strongly attached to the oxygen and the

* Corresponding author.
E-mail address: belkys@fcq.unc.edu.ar (B.A. Maletto).
[1] These authors contributed equally to this work.

http://dx.doi.org/10.1016/j.jconrel.2015.07.008
0168-3659/

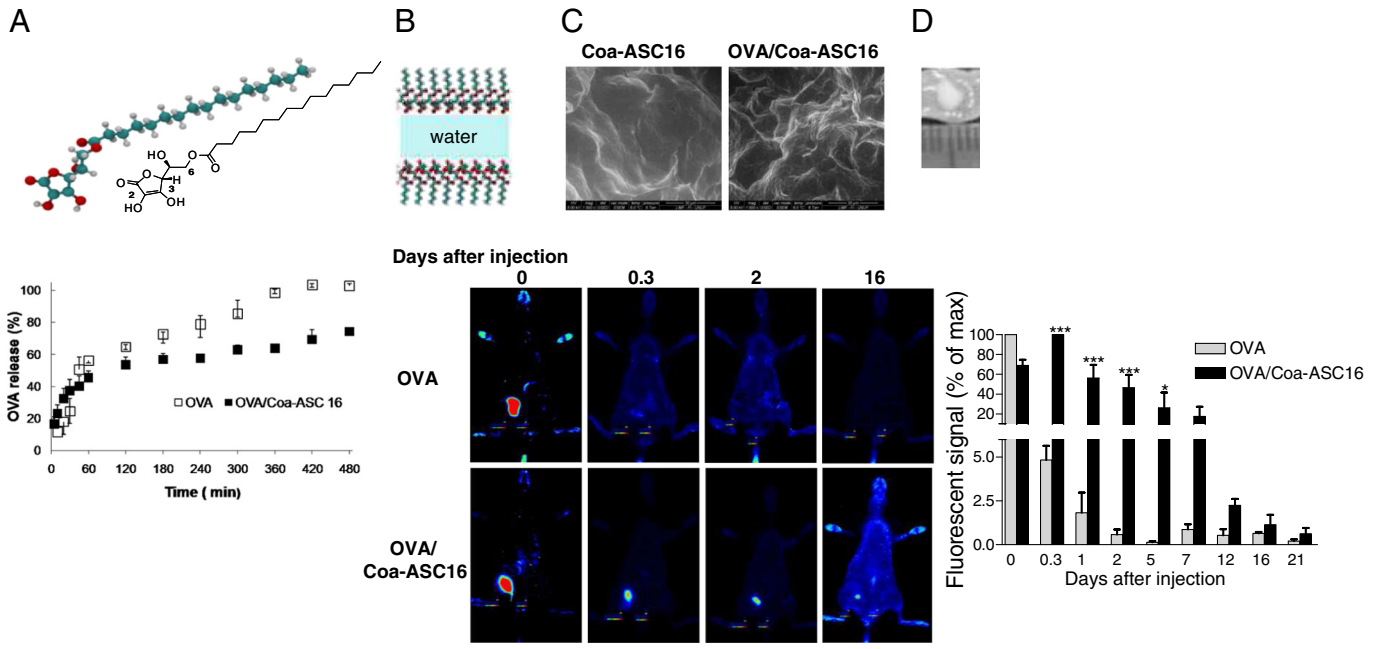

Fig. 1. Characterization of empty and OVA loaded Coa-ASC16. (A) Schematic chemical composition of ASC16. (B) Schematic representation of a hexagonal arrangement of ASC16 forming Coa-ASC16, side view is shown. White, cyan, and red spheres/sticks correspond to hydrogen, carbon, and oxygen, respectively. Water molecules are not shown for clarity. (C) A representative E-SEM picture of Coa-ASC16 and OVA/Coa-ASC16 (1500×). (D) Photograph of Coa-ASC16 nodule retrieved from a mouse 43 h after subcutaneous injection. (E) In vitro release profile of OVA from Coa-ASC16 or dextrose solution over time in buffer Tris–HCl. (F) Mice subcutaneously injected with a solution of dye-OVA in dextrose or dye-OVA formulated with Coa-ASC16 were in vivo imaged in an Odyssey® CLx. On left, fluorescence signal of dye-OVA at the injection sites as a function of time expressed as a percentage of the maximum recorded value. Data show the mean ± SEM and are representative of two independent experiments (3 mice/treatment group in each experiment). On left, representative pseudocolor fluorescent images depict the dye-OVA fluorescence intensity. A higher intensity signal is shown in red, while a lower signal intensity is shown in blue in this heat map display. $^{*}p < 0.05$, $^{***}p < 0.001$.

hydrogen of the –OH groups of the polar headgroups by hydrogen bonds, included in a 3 Å thick layer; the second hydration layer is formed by about 50–60 water molecules per ASC16 one and is extended up to 9 Å from the polar group. Water not included in these two categories behaves as bulk water that surrounds the plate like "islands" and dissolves the few monomers in equilibrium with the coagel phase [3]. Their applications are numerous and we have previously reported that these systems are able to improve the apparent solubility and permeation of certain molecules [4–6], and/or generating in vitro a controlled release [7].

Although protein subunit vaccines are safe, generally they are poorly immunogenic and hence the inclusion of adjuvants is necessary to enhance, direct and maintain antigen-specific immune responses [8]. Only a few adjuvants have been licensed for human use, which include aluminum salts, oil-in-water emulsion (MF59 and ASO3) and 3-O-desacyl-4′-monophosphoryl lipid A (MPL) adsorbed onto aluminum hydroxide (ASO4). When these licensed adjuvants are used with protein subunit antigens, they are able to induce antibody responses. However, these adjuvants are poor at building up protective and durable T cell-mediated immunity, which is crucial for the efficacy of vaccines against intracellular pathogens and cancer [9,10]. Therefore, the development of new adjuvant strategies for protein subunit vaccines is a current important area of investigation in the field of vaccine.

We recently used Coa-ASC16 as a vaccine platform to formulate the model protein antigen ovalbumin (OVA) and the Toll-like receptor (TLR) 9 agonist CpG synthetic oligodeoxynucleotide (CpG-ODN). The latter represents an adjuvant that is part of many successful clinical trials [11], with key features when it is used as a vaccine adjuvant (in contrast with currently licensed adjuvants), including the ability to elicit the polarization of $CD4^+$ T cells toward a T-helper (Th)1 phenotype and, under certain conditions the generation of antigen-specific cytotoxic $CD8^+$ T cell [12,13]. An additional benefit of CpG-ODN is its ability to divert the pre-existing Th2 response in neonates and elderly mice toward a Th1 phenotype [14–17]. However, CpG-ODN still presents some limitations such as a short half-life, unfavorable pharmacokinetics and biodistribution, high binding to plasma protein, a lack of specificity for target cells, poor cellular uptake, and CpG motif-independent side effects that subsequently restrict its clinical application [13,18–20]. Our previous results demonstrated that mice immunized with OVA and CpG-ODN formulated with Coa-ASC16 elicited strong antibodies (IgG1 and IgG2a) and Th1/Th17 cellular responses without toxic systemic effects. These responses were superior to those induced by a solution of OVA with CpG-ODN or OVA/CpG-ODN formulated with aluminum salts. Furthermore, the immunization with OVA/CpG-ODN/Coa-ASC16 resulted in a long-lasting cell-mediated immune response (at least 6.5 months). Taken together, these data indicate that this new adjuvant strategy is an attractive system for promoting an adaptive immune response to emerging weak antigens [7].

It is important to understand the mechanisms of action of adjuvant systems in order to use them rationally and to predict their potential toxicity. However, the mechanisms of action of licensed adjuvants are not well understood. For example, although aluminum salts have been empirically used in vaccines for many decades, their mechanisms of action are still not fully resolved [21]. With respect to our system (antigen and CpG-ODN formulated with Coa-ASC16), we still do not understand exactly how Coa-ASC16 operates in vivo. Previous results from our group obtained by an in vitro release assay suggested that the enhanced specific immune responses elicited when Coa-ASC16 was used as a vaccine platform can be partially attributed to the controlled release of the vaccine components [7]. In addition, in agreement with current evidence that certain biomaterials are not immunologically inert, Coa-ASC16 alone is sensed by the innate immunity triggering an inflammatory response locally at the injection site characterized by leukocyte (neutrophils and $Ly6C^{high}$ monocytes) recruitment and the production of IL-1β, IL-6 and IL-12 [7]. Coa-ASC16 contains no known pathogen-associated molecular pattern (PAMPs) and it is not known how this material stimulates an innate immune response.

The purpose of the present study was to focus on how Coa-ASC16 impacted in vivo on the kinetic of antigen release from the injection

site and to investigate the mechanisms involved in the interaction between Coa-ASC16 and the immune system. To address this last question, we tested the inflammatory response elicited by Coa-ASC16 alone in mice that are deficient in key molecules of the innate immune system. We then studied whether this inflammatory response was associated with an adjuvant effect.

2. Materials and methods

2.1. Mice

WT mice were obtained from the Fundación Facultad de Ciencias Veterinarias (Universidad Nacional de la Plata, La Plata, Argentina), and *Tlr4*$^{-/-}$, *Tlr2*$^{-/-}$, *Myd88*$^{-/-}$ and *Il-6*$^{-/-}$ mice from Jackson Laboratory (Bar harbor, ME). Mice were housed in our animal facility in accordance with the Guide for the Care and Use of Experimental Animals, published by the Canadian Council on Animal Care; with the assurance number A5802-01 delivered by the Office of Laboratory Animal Welfare (National Institutes of Health). *Tlr9*$^{-/-}$, *Ccr2*$^{-/-}$, *Nlrp3*$^{-/-}$ and C57BL/10 mice were obtained from the Centro Nacional de Biotecnología, Madrid, España.

2.2. Reagents

ASC16 was purchased from Fluka Analytical (Milan, Italy) and sterile apyrogenic 5% dextrose solution was obtained from the Laboratorios Roux-Ocefa (Buenos Aires, Argentina). CpG-ODN (sequence 5′-TCCA TGACGTTCCTGACGTT-3′) was synthesized with a nuclease-resistant phosphorothioate backbone (1826, B-class oligodeoxynucleotide) (Operon Technologies, Alameda, CA). The endotoxin content in CpG-ODN after reconstitution, determined by a standard Limulus amebocyte lysate assay (BioWhittaker Inc., Walkersville, MD), was <1 endotoxin unit/mL. TLR9 (IRS 869, 5′-TCCTGGAGGGGTTGT-3) and TLR7 (IRS 661, 5′-TGCTTGCA AGCTTGCAAGCA-3′) inhibitors were synthesized with a nuclease-resistant phosphorothioate backbone and contained no LPS contaminants (Operon Technologies). Both these inhibitors have previously been used for in vivo assays [22,23]. We used DNase I from Sigma-Aldrich (Buenos Aires, Argentina) and OVA from Worthington Biochemical Corporation (Lakewood, NJ). CpG-ODN, DNase I, OVA, IRS 869 and IRS 661 stock solution were prepared in sterile apyrogenic 0.9% NaCl saline solution (B. Braun Medical S.A., Mar del Plata, Argentina). Endotoxins were removed from the OVA stock solution (10 mg/mL) by Detoxi-Gel™ Endotoxin removing columns (Thermo Fisher Scientific Inc., Waltham, MA), and the endotoxin level in the OVA stock solution was determined to be <1 EU/mL using the Endosafe Test (Charles River, Wilmington, MA). To monitor antigen persistence at the injection site in vivo, near-infrared fluorescent dye (IRDye® 680RD) was covalently linked to OVA according to the manufacturer's instructions (LI-COR Biosciences, USA). The use of this system to study in vivo vaccine component delivery has received considerable attention in recent times [24].

2.3. Preparation of Coa-ASC16

ASC16 and 5% dextrose solution were mixed in hermetically closed tubes. This dispersion was heated up to 72 °C (critical micelle temperature) in an ultrasonic bath for 15 min and then left to reach room temperature. In other experiments, IRDye® 680RD OVA or OVA or OVA/CpG-ODN were incorporated into an ASC16/dextrose mixture. In the latter formulations, Coa-ASC16 was prepared using the same method as above. In all cases, the ASC16 concentration was 2% (w/v).

2.4. Observation of the nanostructure by environmental scanning electron microscopy (E-SEM)

Coa-ASC16 and OVA formulated with Coa-ASC16 (OVA/Coa-ASC16) were observed using a FEI ESEM Quanta 200 microscopy (E-SEM working mode: 5 kV, 6 °C and 6 Torr). E-SEM data were obtained at the Servicio de Microscopía Electrónica y Microanálisis (SEMFI-LIMF), Facultad de Ingeniería, Universidad Nacional de la Plata, Argentina.

2.5. In vitro release of OVA from Coa-ASC16

The in vitro release kinetic of OVA from Coa-ASC16 was performed in a modified Franz diffusion cell assembly at 37 ± 1 °C. A Plain sintered disc (17 mm diameter and 5 mm thickness) was placed between the donor and receptor compartment and 1 mL of Coa-ASC16 loaded with OVA (24 μg) or an OVA dextrose solution containing OVA (24 μg) was placed in the donor compartment. The receptor compartment was filled with 4.3 mL of Tris–HCl buffer pH 7.2 and stirred at 200 rpm with a teflon-coated magnetic stirring bar. Periodically, 0.4 mL aliquots were withdrawn and replaced by the same volume of receptor medium. Data were corrected for dilution. The amount of OVA released and present in the receptor compartment was quantified by the Bradford method. All assays were performed in triplicate.

2.6. Antigen persistence at the injection site

Hair from the ventral surface of C57BL/6 mice was removed using depilatory cream. Then, mice were anesthetized by intraperitoneal injection with Ketamine (88 mg/kg)/Xylazine (17 mg/kg) and finally subcutaneously injected in the hind limbs with the different formulations (50 μL/site). In these experiments, IRDye® 680RD OVA was used (1.2 μg/site/mouse). One mice group was injected with a solution of dye-OVA in 5% dextrose in the right hind limb and 5% dextrose in the left hind limb. Another group was injected with dye-OVA formulated with Coa-ASC16 (dye-OVA/Coa-ASC16) in the right hind limb and Coa-ASC16 in the left hind limb. At different time after administration, in vivo scanning of the ventral side of the mice was performed on Odyssey® CLx (LI-COR Biosciences). Scan parameters included resolution: 169 μm; quality: medium; focus offset: 1.0; intensity value: L1 for the 700 nm channel. The fluorescent signal of the injection site was quantified using the Odyssey software package.

2.7. Intraperitoneal injection assay

Mice were injected intraperitoneally with 5% dextrose solution (vehicle) or Coa-ASC16 (50 μL in both cases). At 10 min, 2 or 6 h post-injection, peritoneal lavage was obtained. The peritoneal cavity was washed 3 times with ice-cold HBSS (1 mL per turn) using a plastic Pasteur pipette, and the resulting lavage was centrifuged at 2000 rpm for 5 min in order to separate the supernatant from the cells.

2.8. Flow cytometry

For surface staining, peritoneal cells (1×10^6) were incubated with anti-CD16/32 (2.4G2) (BD Biosciences, Buenos Aires, Argentina) for 15 min at 4 °C and then stained for 30 min at 4 °C with the following antibodies: anti-mouse Ly-6G (1A8), Ly-6C (AL-21), CD11c (HL-3) (all from BD Biosciences) and F4/80 (BM8) (Life Technologies, Buenos Aires, Argentina). Cell subtypes were defined as: macrophage (Ly-6G^{neg} F4/80^{high} Ly-6C^{neg}), neutrophil (Ly-6G^{high} F4/80^{neg} Ly-6C^{+}) and Ly6C^{high} monocyte (Ly6G^{neg} F4/80^{neg} Ly-6C^{high}). For intracellular detection of IL-6 cytokine, peritoneal cells (5×10^5 cell/well) were incubated in a 96-well V-bottom plate (Greiner Bio One, Frickenhausen, Germany) containing GolgiStop (Monensin 4 μL/6 mL) (BD Biosciences) at 37 °C for 4 h. Cells were stained for surface markers before being fixed and permeabilized using the BD Cytofix/Cytoperm™ Plus Kit (BD Biosciences) according to the manufacturer's instructions. Finally, cells were stained for intracellular IL-6 using antibody anti-mouse IL-6 (MPS-20F3) (R&D Systems, Minneapolis, MN) or isotype-matched control antibody for 30 min at 4 °C. For the Annexin/7-AAD assay, peritoneal cells (1×10^5) were resuspended in 100 μL of binding buffer (10 mM Hepes,

pH 7.4, 140 mM NaCl, 2.5 mM $CaCl_2$) and incubated for 15 min at room temperature with 3 μL of Annexin V followed by 1.25 μL of 7-AAD (both from BD Biosciences). Cells were acquired on a FACSCanto II flow cytometer (BD Biosciences) and data were analyzed using FlowJo software (Tree Star).

2.9. Cytokine detection by ELISA

IL-6, IL-12p40, IL17-A and IL-4 cytokines were determined using standard sandwich ELISA. The antibody pairs used were as follows (listed by capture/biotinylated detection): IL-6, MP5-20F3/MP5-32C11 (eBioscience, San Diego, CA); IL-12p40, C15.6/C17.8 (BD Biosciences); IL-17A, 17CK15A5/17B7 (eBioscience); IL-4, 11B11/BVD6-24G2 (BD Biosciences). The ELISA Ready-SET-Go!® kit for IL-1β cytokine detection was purchased from eBioscience and the BD OptEIA mouse IFN-γ ELISA Set for IFN-γ from BD Biosciences, with both being used according to the manufacturer's instructions.

2.10. In vitro DNase treatment and DNA quantification

The peritoneal lavage supernatant was incubated with DNase I (5 μg/mL) and $MnCl_2$ (0.01 M) (both at final concentration) for 45 min at 37 °C. This reaction was stopped by adding EDTA (25 mM as final concentration). dsDNA was quantified by Quant-iT dsDNA BR Assay Kit (Life Technologies) under the established manufacturer's protocols.

2.11. Determination of the concentrations of ALT, AST and LDH

These assays were performed using an enzymatic standard biochemical kit (Wiener Lab, Rosario, Argentina) under the established manufacturer's protocols.

2.12. Immunizations

Mice were subcutaneously immunized with a solution of OVA, OVA/Coa-ASC16 or OVA and CpG-ODN formulated with Coa-ASC16 (OVA/CpG-ODN/Coa-ASC16). Immunizations were performed at days 0, 7 and 14. Each mouse was immunized with an entire dose (250 μL) equally distributed at five sites: tail, back, neck region and both hind limbs (50 μL/site). The OVA dose injected was 6.6 μg/mouse/dose. CpG-ODN was administered at 75 μg/mouse/dose.

2.13. Splenocyte preparation and ex vivo restimulation

Spleen cell suspensions were obtained after lysing the red blood cells using the RBC lysing buffer (Sigma-Aldrich). Splenocytes (1×10^6 cell/well) were incubated for 72 h in a 96-well U-bottom plate (Greiner Bio One) with medium or OVA (100 μg/mL) at 37 °C and 5% CO_2. The GIBCO® RPMI 1640 medium (Life Technologies) was used supplemented with 10% heat-inactivated fetal bovine serum (PAA Laboratories GmbH, Linz, Austria), 2 mM GIBCO® Glutamax, 100 U/mL penicillin, 100 μg/mL streptomycin (all from Life Technologies) and 50 μM 2-mercaptoethanol (Sigma-Aldrich). Supernatants were collected at 72 h to determine cytokine production by ELISA.

2.14. Specific-OVA antibody titers by ELISA

The *specific-OVA antibody titers were* measured *by ELISA* according to [7]. The antibodies used were HRP-conjugated anti-mouse IgG1 (X56) and IgG2a/c (R19-15) (both from BD Biosciences). Titer was considered to be the reciprocal of the last plasma dilution that yielded an absorbance value 490 nm greater than that of twice the mean value of blank. The plasmas from non-immunized mice were not reactive to OVA.

2.15. Statistical analysis

Statistics were performed using GraphPad Prism software. The one-way ANOVA followed by Bonferroni post-test selected comparisons and the unpaired Student's t- test were used. p values <0.05 were considered significant.

3. Results

3.1. Characterization of empty and OVA loaded Coa-ASC16

Coagels are made up of densely packed lamellar layers of surfactants interlocked by hydrophilic regions that contain a specific amount of strongly bound water molecules [2]. We studied the ultrastructure of coagels by E-SEM. An E-SEM micrograph of Coa-ASC16 (Fig. 1C) confirmed the presence of a 3D-network of entangled crystalline plates that entrapped water. This 3-D network was clearly a consequence of the rapid growth of rigid plates from the gel at the critical micelle temperature [25]. In this sense, the water structure played a key role related to the coagel self-aggregation. A representative E-SEM picture of OVA antigen formulated with Coa-ASC16 is also shown in Fig. 1C with no changes being observed in the lamellar structure, suggesting that OVA is in the aqueous environment of the coagel.

Coa-ASC16 revealed a homogeneous appearance, and no phase separation was observed over a period of at least 15 days (data not shown), thus indicating that it is temporally stable. Coa-ASC16 appeared as white, rather soft curds, with a node being formed immediately after subcutaneous injection in mice. In Fig. 1D, the nodule retrieved at 43 h after injection is shown. Next, the in vitro release profile of OVA from Coa-ASC16 was studied and Fig. 1E reveals that Coa-ASC16 controls the OVA release pattern.

To attempt to unravel the underlying mechanisms that enhanced the immune responses in vivo elicited by Coa-ASC16, we investigated antigen persistence at the injection site. To carry this out, the duration of dye-OVA at the vaccine site was compared after subcutaneous injection of dye-OVA solution or dye-OVA formulated with Coa-ASC16, using in vivo near-infrared fluorescent imaging (Fig. 1F). In mice injected with soluble dye-OVA, within 0.3 days the fluorescence signal at the injection site decreased to less than 5% of its initial value, indicating that unformulated protein was cleared rapidly from the injection site. In contrast, dye-OVA formulated with Coa-ASC16 was removed from the injection site more gradually remaining there for several days. This result suggests that Coa-ASC16 effectively serves in vivo as a depot (slow sustained release of loaded molecules) to maintain the antigen at the site of injection, thereby prolonging its interaction with the immune system.

3.2. Study of inflammatory events triggered by Coa-ASC16 in MyD88- or TLR-deficient mice

We have previously shown that Coa-ASC16 alone parenterally administered induces a local inflammatory response at the injection site [7]. Here, we examined how Coa-ASC16 interacts with the innate immune system. In order to evaluate this, WT or knockout mice were intraperitoneally injected with Coa-ASC16 or dextrose (control group) and then peritoneal lavages were analyzed. Coa-ASC16 promoted in WT mice cellular recruitment initiated by neutrophils (2 h after injection) followed by $Ly6C^{high}$ monocytes (6 h after injection), with this leukocyte infiltrate being accompanied by IL-1β (detected in all experiments at 2 h and in some experiments also at 6 h), IL-6 and IL-12 (both detected at 2 h and 6 h) (Fig. 2). Prior studies have reported that some materials that did not contain any known PAMPs (aluminum salts, MF59, nitrogen bisphosphonates or ISCOMATRIX) were able to activate the immune system through a mechanism that required MyD88, a critical adaptor protein in innate immunity [26–29]. MyD88 adaptor protein mediates TLR and IL-1R receptor families signaling [30].

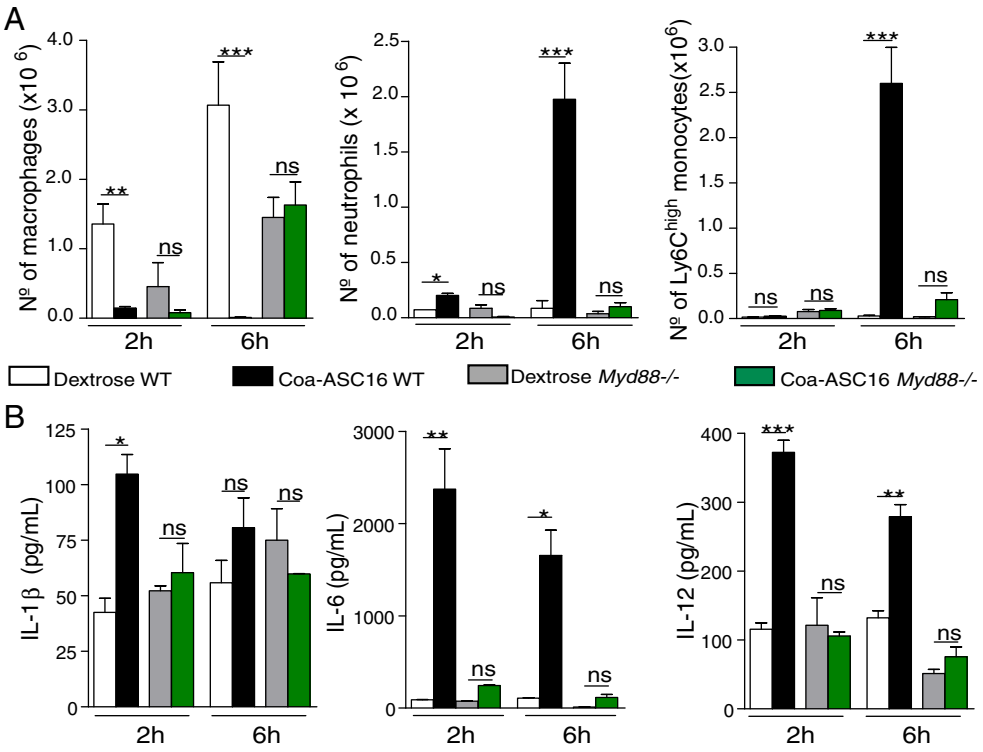

Fig. 2. Lack of MyD88 in mice impairs the recruitment of neutrophils and Ly6C^{high} monocytes and also the production of cytokines elicited after Coa-ASC16 administration. Mice were intraperitoneally injected with dextrose or Coa-ASC16, and the peritoneal cavity was analyzed 2 or 6 h post-injection. (A) Number of macrophages, neutrophils and monocytes. (B) Concentrations of IL-1β, IL-6 and IL-12 measured by ELISA in the supernatant of peritoneal lavage. Data show the mean ± SEM and are representative of three/four independent experiments (3–4 mice/treatment group in each experiment). $^{*}p < 0.05$, $^{**}p < 0.01$, $^{***}p < 0.001$, ns: not significant.

Therefore, we examined how MyD88 deficiency affects inflammatory events elicited by Coa-ASC16. Our results revealed that Myd88$^{-/-}$ mice had reduced leukocyte recruitment and cytokine production (IL-1β, IL-6 and IL-12) in response to Coa-ASC16 (Fig. 2).

Next, we decided to focus on the study of the innate response observed at 6 h after injection of Coa-ASC16 and investigate the pathways contributing to this response. Thus, we tested the impact of TLR signaling on the Coa-ASC16-mediated inflammatory response. We found that the *Tlr2*$^{-/-}$, *Tlr4*$^{-/-}$ mice, and those pretreated with TLR7 inhibitor (IRS 661) were able to induce an inflammatory response that was triggered after Coa-ASC16 administration (Supplementary Figs. 1 and 2), thereby indicating that TLR2, TLR4 and TLR7 were not involved in these events. In addition, in *Tlr9*$^{-/-}$ mice (Fig. 3) or in mice pretreated with TLR9 inhibitor (IRS 869) (Supplementary Fig. 3), leukocyte recruitment was not modified. In contrast, we found in *Tlr9*$^{-/-}$ mice as in mice pretreated with IRS 869 that the IL-6 and IL-12 production was abolished after Coa-ASC16 injection (Fig. 3 and Supplementary Fig. 3).

Taken together, these findings demonstrate that MyD88 adaptor protein is indispensable for a Coa-ASC16-mediated inflammatory response. Moreover, the production of IL-6 and IL-12 is a consequence of TLR9-dependent signaling.

3.3. Evaluation of recruitment of LyC6^{high} monocytes induced by Coa-ASC16 in IL-6-deficient mice

Many different cell types, including those derived from bone-marrow as well as stromal cells, have been identified as sources of IL-6. Furthermore, there are several lines of evidence suggesting that IL-6 plays a pivotal role during the transition from innate to acquired immunity [31].

Considering that Coa-ASC16 triggered a robust production of IL-6 and that innate cells accumulated at the injection site, we searched for potential sources of IL-6 and found that all the neutrophils and half of the Ly6C^{high} monocytes produced IL-6 (Fig. 4A).

Coa-ASC16 induces an inflammatory response characterized by an initial infiltration of neutrophils, which is then followed by Ly6C^{high} monocytes. Prior studies reported that the IL-6/soluble IL-6Rα complex can mediate the transition from neutrophil to monocyte accumulation in inflammation [32]. Therefore, we examined how IL-6 deficiency affects the recruitment of monocytes induced by Coa-ASC16 injection. Notably, in our study, the analysis of peritoneal inflammation in *Il-6*$^{-/-}$ mice revealed that IL-6 was not necessary for Ly6C^{high} monocyte influx after injection of Coa-ASC16 (Fig. 4B–C).

3.4. Study of inflammatory events triggered by Coa-ASC16 in CCR2-deficient mice

It has been previously shown that Ly6C^{high} monocytes cannot egress from the bone marrow in the absence of the CCR2 chemokine receptor [33]. To determine whether Ly6C^{high} monocytes could influence the profile of the cytokine response induced by Coa-ASC16, the *Ccr2*$^{-/-}$ mice were injected with Coa-ASC16. It was found that neutrophils were recruited into the peritoneum of WT and *Ccr2*$^{-/-}$ mice, whereas Ly6C^{high} monocytes were only recruited in WT mice. At the same time, the absence of Ly6C^{high} monocytes in the peritoneum correlated with lower concentrations of IL-6 and IL-12 in *Ccr2*$^{-/-}$ mice compared with WT mice (Fig. 4D–E). Collectively, these results indicate that in our experimental model, CCR2-signaling contributed to the recruitment of Ly6C^{high} monocyte at the injection site, and they also reveal a role for Ly6C^{high} monocytes in IL-6 and IL-12 production.

3.5. In vivo DNase treatment reduces IL-6 and IL-12 production elicited by Coa-ASC16

Coa-ASC16 is formed by ASC16, an amphiphilic molecule that behaves as a surfactant. Due to the fact that this nanostructure can interact with biological and model membranes [34,35], we postulated that this

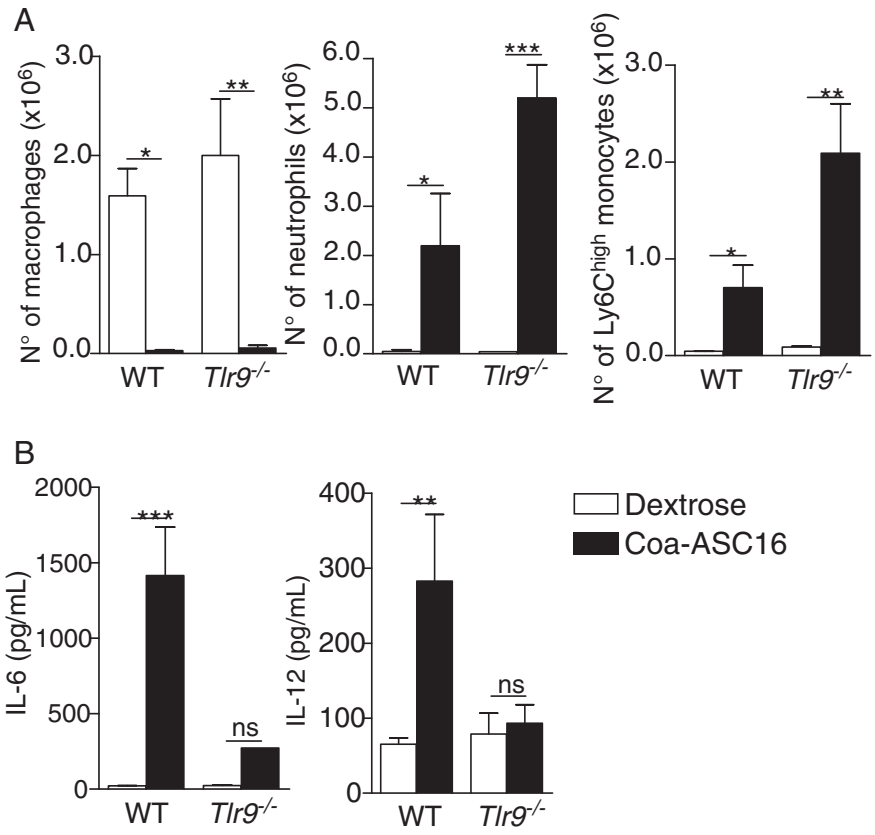

Fig. 3. *Tlr9*$^{-/-}$ mice are not able to induce IL-6 and IL-12 after Coa-ASC16 administration. Mice were intraperitoneally injected with dextrose or Coa-ASC16 and the peritoneal cavity was analyzed 6 h post-injection. (A) Number of macrophages, neutrophils and monocytes. (B) Concentrations of IL-6 and IL-12 measured by ELISA in the supernatant of peritoneal lavage. Data show the mean ± SEM and are representative of two independent experiments (3–4 mice/treatment group in each experiment). *$p < 0.05$, **$p < 0.01$, ***$p < 0.001$, ns: not significant.

interaction might be generating cellular damage at the injection site. Therefore, we performed a cell viability assay and found that Coa-ASC16 induced cell death ($7AAD^+$ $AnnexinV^-$ cells) (Fig. 5A) associated with a transient decrease in the number of total leukocytes (Fig. 5B). At the same time, a temporary accumulation of the intracellular proteins alanine aminotransferase (ALT), aspartate aminotransferase (AST) and lactate deshidrogenase (LDH) was detected in the cell-free supernatant of the peritoneal lavage (Fig. 5C). This cell death was correlated with a transient accumulation of double-stranded DNA (dsDNA) in the cell-free supernatant of the peritoneal lavage, which was reduced by treating the samples in vitro with DNase, thus revealing the specificity of the method used (Fig. 5D). In addition, the treatment of mice with DNase impaired the production of IL-6 and IL-12 but not the cell recruitment triggered by Coa-ASC16 (Fig. 5E–F), similar to the pattern shown previously in *Tlr9*$^{-/-}$ mice (Fig. 3). These findings demonstrate that Coa-ASC16 induced local cell death and consequently dsDNA release at the injection site. In conclusion, the host DNA, which acted as a damage-associated molecular pattern (DAMP) associated with TLR9, mediated IL-6 and IL-12 secretion after administration of Coa-ASC16.

3.6. Study of inflammatory events triggered by Coa-ASC16 in NLRP3-deficient mice

The NLRP3 inflammasome is activated in response to infectious stimuli or to a wide range of DAMPs [36] and has also been shown to be related to the mechanism of action of some adjuvants that do not contain known PAMPs [37]. We hypothesize that there could be a link between NLRP3 inflammasome and the inflammatory activity of Coa-ASC16. However, we found that injection of *Nlrp3*$^{-/-}$ mice with Coa-ASC16 triggered an inflammatory response as efficiently as in WT mice (Supplementary Fig. 4). This finding demonstrates that NLRP3 inflammasome was not critical for the generation of the inflammatory response observed at 6 h after Coa-ASC16 injection.

3.7. Comparison of antigen-specific response in mice immunized with OVA vs mice immunized with OVA formulated with Coa-ASC16

The mechanisms of action of vaccine adjuvants are poorly understood. In some case, the success of some vaccine adjuvants consists in the recruitment of innate immune cells at the site of injection and the subsequent priming of the adaptive immune system (adjuvant effect) [38]. To investigate if this occurs with Coa-ASC16, we decided to study if it has intrinsic adjuvant activity alone. Therefore, mice were subcutaneously immunized with OVA alone or formulated with Coa-ASC16 and the formulation OVA/Coa-ASC16 triggered antigen-specific IgG1, IgG2c and IFN-γ production in WT mice (Fig. 6A–B). Recently, we have introduced Coa-ASC16 as a platform for CpG-ODN and OVA, as it has the ability to induce strong antigen-specific antibodies (IgG1 and IgG2a/c) and Th1/Th17 cellular responses in mice [7]. Here, we show that WT mice immunized with OVA/CpG-ODN/Coa-ASC16 exhibited significantly stronger titers of OVA-specific IgG2c compared with the WT mice immunized with OVA/Coa-ASC16 ($p < 0.001$) (Fig. 6A). In addition, immunization with OVA/CpG-ODN/Coa-ASC16 induced a Th17 cellular response [7] but this response was not seen in WT mice immunized with OVA/Coa-ASC16 (data not shown).

Since the inflammatory activity of Coa-ASC16 depends on MyD88 adaptor protein, next we investigated whether MyD88 was required for a Coa-ASC16 adjuvant effect. Although, immunization of *Myd88*$^{-/-}$ mice with OVA/Coa-ASC16 did not induce anti-OVA IgG2c or IFN-γ production, *Myd88*$^{-/-}$ mice were able to develop OVA-specific IgG1 (Fig. 6A–B).

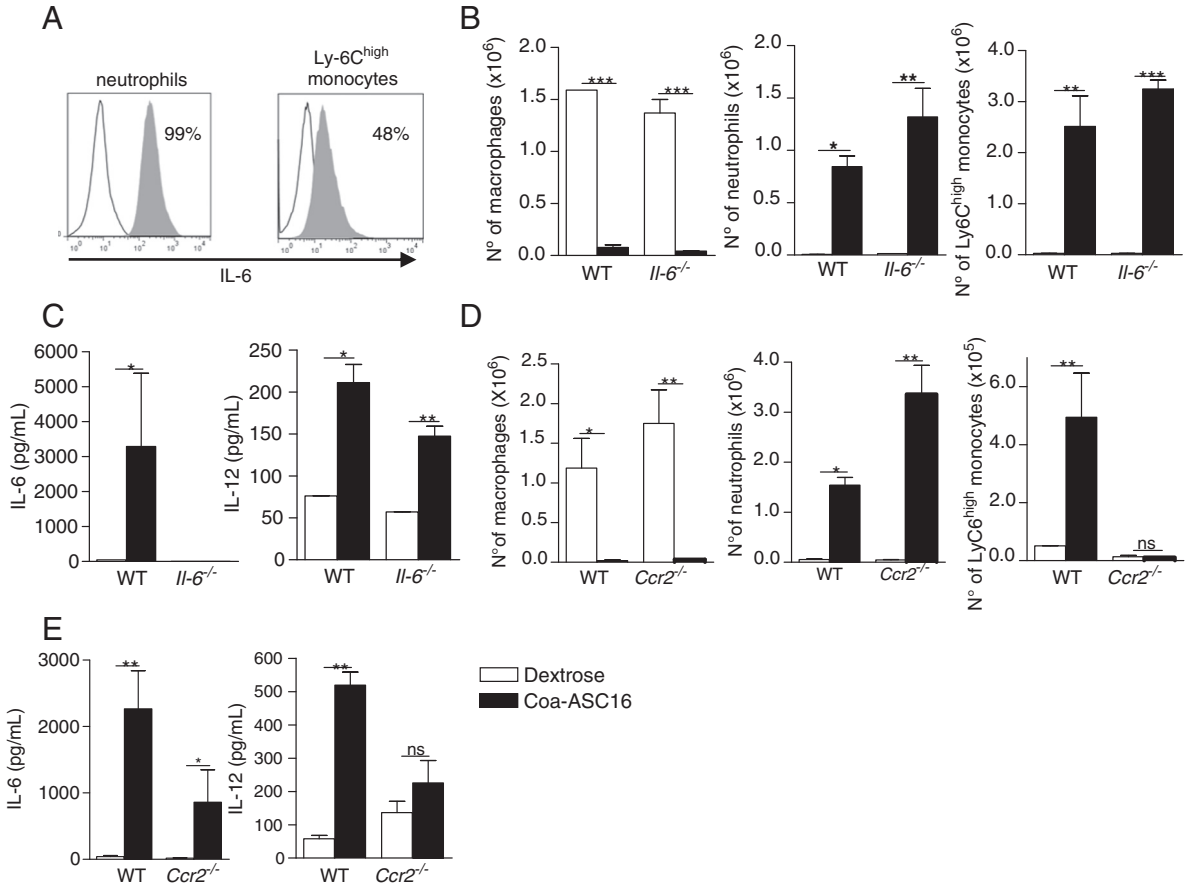

Fig. 4. IL-6 is not required for monocyte recruitment, and in *Ccr2*$^{-/-}$ mice there is an impaired production of IL-6 and IL-12 after Coa-ASC16 administration. Mice were intraperitoneally injected with dextrose or Coa-ASC16 and the peritoneal cavity was analyzed at 6 h post-injection. (A) Intracellular IL-6 staining by flow cytometry. The dark histograms show expression of intracellular IL-6 in a gated population and line histograms represent isotype control, with the number indicating the frequency of IL-6^{+} cells in the gated population. (B and D) Number of macrophages, neutrophils and monocytes. (C and E) Concentrations of IL-6 and IL-12 measured by ELISA in the supernatant of peritoneal lavage. Data show the mean ± SEM and are representative of three independent experiments (3–4 mice/treatment group in each experiment). *$p < 0.05$, **$p < 0.01$, ***$p < 0.001$, ns: not significant.

Next, we tested the adjuvant activity of Coa-ASC16 in mice deficient in TLR4, and the adjuvant activity of Coa-ASC16 was found to be independent of TLR4 signaling (Supplementary Fig. 5).

Coa-ASC16 promotes a robust production of IL-6. To determine whether IL-6 has a role in the adaptive response induced by Coa-ASC16, mice deficient in this cytokine were immunized with OVA or OVA/Coa-ASC16. The *Il-6*$^{-/-}$ mice failed to produce anti-OVA IgG2c after OVA/Coa-ASC16 immunization (Fig. 6C). Collectively, these results demonstrate that Coa-ASC16 alone has adjuvant activity, with MyD88 protein and IL-6 being partially required for Coa-ASC16 adjuvanticity.

4. Discussion

Coa-ASC16 has the following advantages that make it a very attractive platform for biomedical use: (i) it is comprised of a single molecule of an ester formed from ascorbic acid and palmitic acid, which are both biodegradable molecules; (ii) ascorbic acid preserves its antioxidant property [39]; (iii) ASC16 is listed as a Generally Recognized as Safe (GRAS) substance; (iv) it is easy to prepare and inexpensive.

Although, we have previously described that the injection of antigen/CpG-ODN formulated with Coa-ASC16 enhances specific immune responses compared to antigen/CpG-ODN in solution [7], the exact mechanism of action of Coa-ASC16 is still unknown [7]. In the present study, we investigated how Coa-ASC16 operates in vivo when used as a vaccine platform.

Our results indicate that the antigen was slowly released from Coa-ASC16, not only under in vitro conditions but also at the injection site of the mice (Fig. 1E–F). It is well known that prolonged exposition of antigen to immune cells is propitious to inducing powerful immune responses. Additionally, this in vivo release behavior of antigen from Coa-ASC16 may have an impact on the biodistribution results of all vaccine components, which requires further research to resolve this issue.

We had been surprised when our previous studies had shown that Coa-ASC16 injected alone (without antigen) was sensed by the innate immune system triggering, per se, an early inflammatory response at the injection site [7]. Here, we have reported that Coa-ASC16 has an inflammatory effect associated with a self adjuvanticity property. It is possible that this adjuvanticity property of Coa-ASC16 contributes to enhance adjuvant activity of CpG-ODN. Although Coa-ASC16 alone is sufficient to act as an adjuvant, we found that the formulation CpG-ODN/Coa-ASC16 is much better than Coa-ASC16 at inducing anti-OVA IgG2c (Fig. 6A) and the Th17 cell response [7], thus supporting distinct immunogenic mechanisms for these two adjuvant strategies. In this way, these findings show how different adjuvant strategies trigger different profiles of the adaptive immune response, thus offering the possibility to select one according to the required response. Taking all these results into consideration, the present study suggested that Coa-ASC16 improves vaccine efficacy by a combination of various mechanisms, including induction of an adequate immunocompetent environment and an antigen depot at the injection site.

It has been shown that some adjuvants induce early immune cell recruitment and cytokine milieu at the injection site. However, the relationship between this phenomena and adjuvant activity is still unclear [38]. Here, we have shown that both Coa-ASC16 inflammatory activity and its adjuvant effect depend on MyD88 signaling, with IL-6 appearing to be one of the molecules that can create a link between both responses

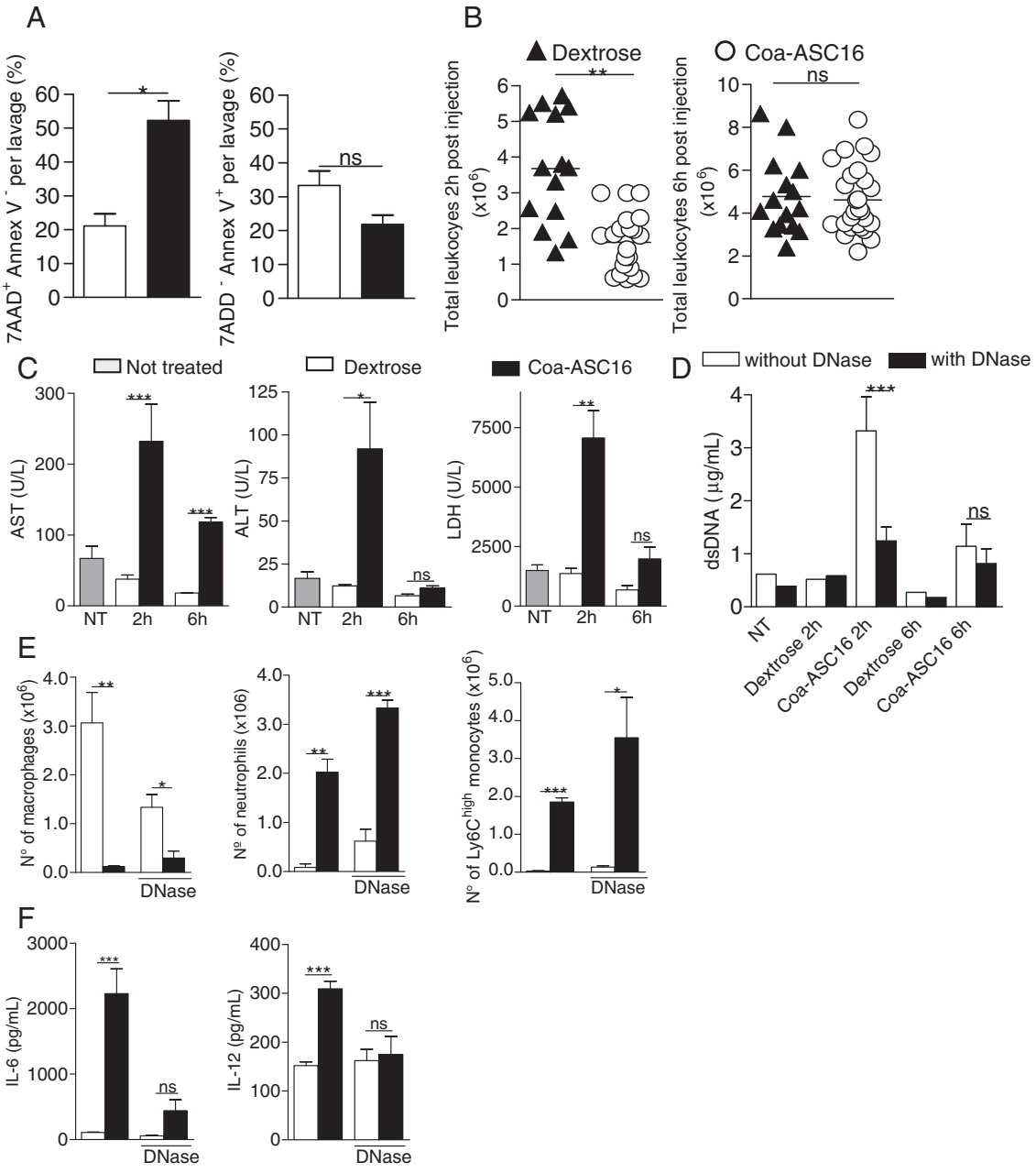

Fig. 5. In vivo pretreatment of mice with DNase enzyme impairs the production of IL-6 and IL-12 triggered by Coa-ASC16. (A–D) Mice were intraperitoneally injected with dextrose or Coa-ASC16 and the peritoneal cavity was analyzed. (A) Cell viability study. Bars show the percentage of 7-AAD$^+$ Annex V$^-$ or 7-AAD$^-$ Annex V$^+$ cells in the peritoneal cavity 10 min after injection, assessed by flow cytometry. (B) Number of total leukocytes in peritoneal cavity 2 h and 6 h after injection. (C) Peritoneal lavage supernatant concentrations of AST, ALT and LDH measured at 2 h and 6 h after injection. (D) Concentration of dsDNA in peritoneal lavage supernatants at 2 h and 6 h after injection, with or without prior treatment in vitro with DNase I enzyme. (E–F) Mice were intraperitoneally injected with 1 mg of DNase I enzyme 10 min before dextrose or Coa-ASC16 intraperitoneal injection, and the peritoneal cavity was analyzed at 6 h post-injection. (E) Number of macrophages, neutrophils and monocytes, and (F) Concentrations of IL-6 and IL-12 measured by ELISA in the supernatant of peritoneal lavage. Data show the mean ± SEM and are representative of two/three independent experiments (3–4 mice/treatment group in each experiment). *$p < 0.05$, **$p < 0.01$, ***$p < 0.001$, ns: not significant.

with its production requiring dsDNA (Fig. 5F). Therefore, these results provide strong evidence that host DNA is a crucial molecule for adjuvant activity of Coa-ASC16. Related to this, previous studies have implicated endogenous molecules such as uric acid, host DNA and ATP in the adjuvanticity of aluminum salts and MF59 [26,40–42]. To our knowledge, this is one of the first studies where a causal relationship between an inflammatory response and adjuvant activity has been demonstrated.

The inflammatory response induced by Coa-ASC16 was entirely abrogated in *Myd88*$^{-/-}$ mice (Fig. 2). MyD88 is a critical apical adaptor protein in the signal transduction of most TLRs (except TLR3) and receptors of the IL-1 cytokine family [30]. Here, we determined that the inflammatory response does not require TLR2, TLR4 or TLR7 signaling (Supplementary Figs. 1 and 2), but notably, TLR9 signaling was involved in IL-6 and IL-12 production but not in cell recruitment (Fig. 3). Since TLR2 pairs with TLR1 and TLR6, TLR4 pairs with TLR6, TLR5 binds flagellin, TLR8 is non-functional in mice, TLR11/TLR12 respond to T. gondii profilin, and TLR13 responds to a defined sequence of the bacterial rRNA, we consider that TLR-dependent signaling has been fully evaluated. However, we cannot exclude that members of IL-1R family may contribute to Coa-ASC16 action since this was not evaluated in this investigation. Future studies are required to elucidate this aspect. In fact, Coa-ASC16 is formed by an ester, which to date has not been described as a PAMP. Nevertheless, it has been previously shown that one of its

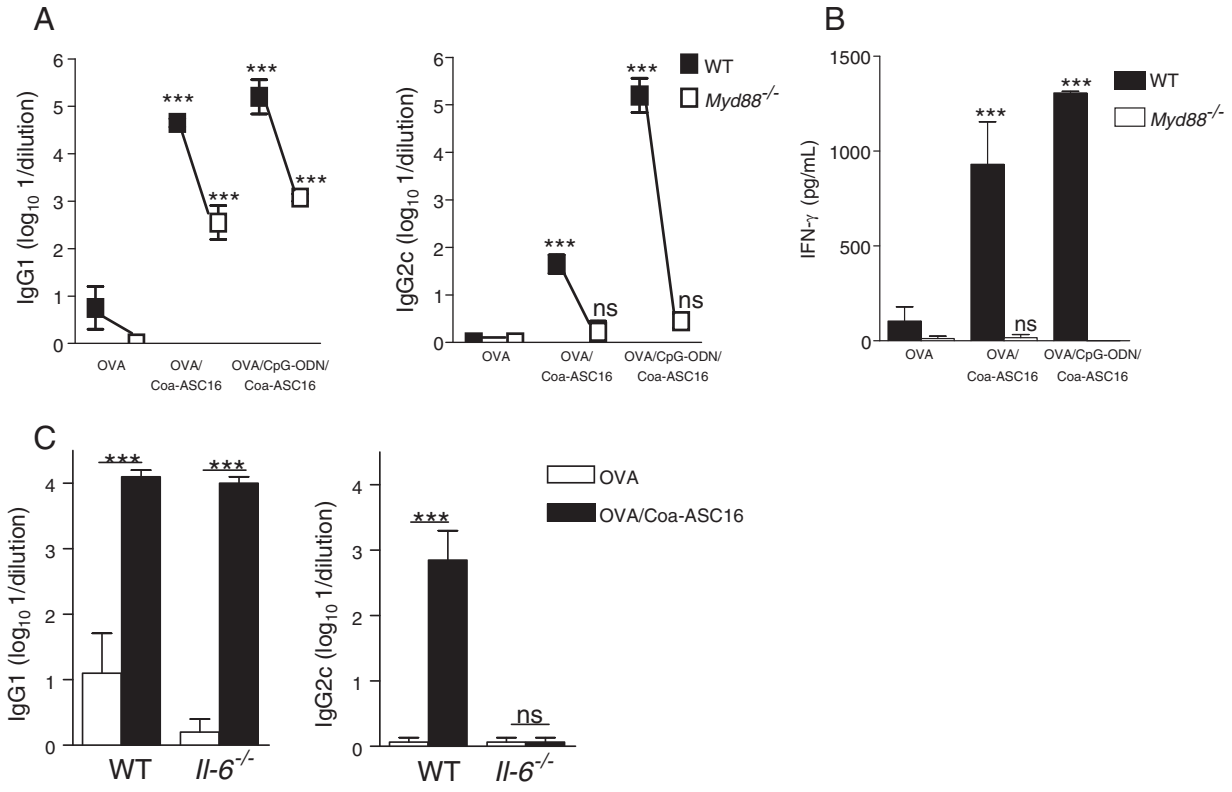

Fig. 6. Adjuvant activity of Coa-ASC16 depends on MyD88 and IL-6. Mice were subcutaneously immunized at days 0, 7 and 14 with OVA, OVA/Coa-ASC16 or OVA/CpG-ODN/Coa-ASC16. At day 21 after the first immunization, plasma and spleen were obtained. (A and C) OVA-specific IgG1 and IgG2c titers. (B) OVA-specific IFN-γ production by splenocytes was examined by ELISA. OVA-specific cytokine production was calculated by subtracting cytokine production measured in the absence of OVA from that in the presence of OVA. Data show the mean ± SEM and are representative of two independent experiments (3–4 mice/treatment group in each experiment). In (A–B), ns: not significant or ***$p < 0.001$ comparing OVA/Coa-ASC16 or OVA/CpG-ODN/Coa-ASC16 with OVA in WT or *Myd88*$^{-/-}$ mice. In (C) ns: not significant or ***$p < 0.001$ comparing OVA/Coa-ASC16 with OVA in WT or *Il-6*$^{-/-}$ mice.

components, palmitic acid, can activate TLR2 and TLR4 [43–45]. In contrast, our results indicate that neither TLR2 nor TLR4 was involved in the inflammatory response induced by Coa-ASC16.

The results of our study provide strong evidence that the innate immune response observed post Coa-ASC16 injection was triggered at least in part by an indirect mechanism mediated by dsDNA (a DAMP), with perhaps other DAMPs also being involved in its action. Peritoneal cells exposed to Coa-ASC16 underwent a cell-death response, which we propose initiated inflammatory events at the injection site. This probably resulted as this nanostructure has the ability to interact with the erythrocyte membrane and phospholipid monolayer [34,35]. Closely related to this, Flach et al. reported that aluminum salt interaction with dendritic cell membrane lipids is essential for its adjuvanticity [46].

Previously, other authors have shown that in mice immunized with T-dependent antigen plus TLRs agonists, the IFN-γ production by T cells and the switching to IgG2a/c is dependent on MyD88 signaling [47,48]. Here, we have demonstrated that MyD88 is necessary for both the innate and adaptive immune responses elicited by Coa-ASC16 (Figs. 2 and 6). If the adjuvant mechanism of Coa-ASC16 had been completely due to the activation of the MyD88-dependent innate immunity, then this response would have been expected to have been totally abrogated in the absence of MyD88. However, *Myd88*$^{-/-}$ mice immunized with OVA/Coa-ASC16 revealed that although the loss of MyD88 markedly reduced anti-OVA IgG2c and IFN-γ production, some adjuvant activity was still maintained particularly for the generation of anti-OVA IgG1 (Fig. 6A), thus indicating an additional role of a non-MyD88-dependent adjuvant effect. This result was not unexpected because in addition to the activation of the innate immunity, Coa-ASC16 also prolonged antigen availability at the injection site. Other studies have reported that adjuvants that do not contain known PAMPs act through a mechanism that requires MyD88 to induce an adaptive immune response, with our results being in agreement with some of these data. Seubert et al. reported that the antigen-specific IgG1, IgG2b/c, and IgG3 production induced by MF59 (an oil-in-water emulsion that consists of squalene oil, citrate buffer, and two non-ionic surfactants) and IgG2b induced by aluminum salts were all affected by a MyD88 deficiency [27]. Similarly, Wilson et al. showed that cellular immunity was impaired in *Myd88*$^{-/-}$ mice immunized with an ISCOMATRIX adjuvant (a saponin, phospholipid and cholesterol components-based particulate adjuvant) [29]. In addition, our data obtained with *Tlr4*$^{-/-}$ mice (Supplementary Figs. 1 and 5) indicate that our formulation was not contaminated with endotoxin.

The innate immunity profiles developed by Coa-ASC16 in mice pretreated with DNase and TLR9 inhibitor were similar to those in *Tlr9*$^{-/-}$ mice (Fig. 5E–F, Supplementary Fig. 3 and Fig. 3). In all cases, there was a deficiency in the production of IL-6 and IL-12 cytokines but no impact on cell recruitment. Host dsDNA activates signaling pathways initiated by different receptors such as endosomal TLR9 via the adaptor protein MyD88 [49,50] and several cytosolic sensors that signal through the STING adaptor protein [51]. The results presented here show that in our experimental model the TLR9-dependent pathway was involved in the action of dsDNA. In contrast, dsDNA release by other adjuvants such as aluminum salts operates following activation of cytosolic sensors, because of the ability of aluminum salts to deliver host DNA to the cytosol [40,41]. However, in the case of Coa-ASC16, this probably does not occur, with it being very likely that dsDNA reaches a high concentration in the extracellular space as a result of its release by dead cells and possibly does not reach the cytoplasm. According to our knowledge this is the first report that shows a liquid crystal nanostructure that has immune stimulatory effects able to activate the TLR9 pathway (through the release of DNA).

Several studies have shown NLRP3 inflammasome activation in response to adjuvants that do not contain known PAMPs. However, there are some conflicting results related to the involvement of NLRP3 inflammasome in vivo adaptive immunity, for example, in the role of NLRP3 inflammasome in the adjuvant activity of aluminum salts [37]. Here, we have shown that the inflammatory response induced at 6 h after Coa-ASC16 injection was NLRP3 inflammasome-independent. This was probably due to mature IL-1β being produced by other inflammasomes or by additional enzymes, including, proteases such as proteinase-3, elastase and granzyme A [52]. However, this possibility is still awaiting resolution.

There are several lines of evidence suggesting that IL-6 (one of the most pleiotropic cytokines) plays a pivotal role during the transition from innate to acquired immunity [31,53], which has resulted in the growing interest in studying the role of IL-6 on adjuvant efficacy. Coa-ASC16 promotes a robust production of IL-6, with the production of this cytokine being specific to a dsDNA stimulus and completely dependent TLR9 signaling (Figs. 5F and 3). In our system, IL-6 deficiency had no impact on the recruitment of Ly6C^{high} monocytes (Fig. 4B), but had a profound effect on the antigen-specific IgG2c titers (the isotype regulated by IFN-γ), while the titers of antigen-specific IgG1 were not reduced (Fig. 6C). This last observation is consistent with a report by Hui et al., where the authors demonstrated that MPL-type adjuvants induced lower levels of IgG2a in *Il-6*$^{-/-}$ mice compared with WT mice. However, the addition of QS21 (a saponin derivative) into the formulation restored the ability to produce IgG2a in *Il-6*$^{-/-}$ mice at comparable levels to those observed in WT mice. In contrast, *Il-6*$^{-/-}$ mice receiving MF59 had antibody titers significantly higher in IgG1 but with less IgG2a than WT mice [54]. Interestingly, Nish et al. recently showed that a defective IL-6 signaling in CD4^{+} T cells affected predominantly the titers of IgG2c, while the titers of IgG1 were only modestly reduced after immunization with OVA and LPS in IFA [53]. Taken together, these results show that an adjuvant may rely on one of the biological activities of IL-6 more than another adjuvant formulation, depending on its ability to drive compensatory pathways.

5. Conclusions

The results of this work highlight new insights regarding the manner in which Coa-ASC16 works. We have shown here that Coa-ASC16 created an antigen depot and immunocompetent environment at the injection site. Our results also indicate that this immunocompetent environment is mediated at least in part by TLR9 (through the release of self DNA). In addition, we found that Coa-ASC16 presents an adjuvant activity associated with its inflammatory effect, with both depending on the MyD88 adaptor protein. IL-6 cytokine linked the innate and adaptive immune responses, thus Coa-ASC16 has not only a platform capacity but also exhibits an intrinsic adjuvant property when administered by the parenteral via. This improved understanding of how Coa-ASC16 operates could allow this novel vaccination tool to be used in a more rational way. Our results are particularly relevant in the current context, where it has been found that some biomaterials are not immunologically inert and therefore may be possible candidates for use as adjuvants.

Supplementary data to this article can be found online at http://dx.doi.org/10.1016/j.jconrel.2015.07.008.

Acknowledgments

We thank Dr. P. Abadie, Dr. P. Crespo, A. Romero and Dr. I. Crespo for technical assistance; F. Navarro and L. Navarro for animal care; Dr. I. Couillin (CNRS and University of Orleans) for providing *Nlrp3*$^{-/-}$ mice; Dr. J. Pardo (University of Zaragoza) for supplying *Tlr9*$^{-/-}$ mice; Dr. F. J. Arias (University of Valladolid) for quantifying the endotoxin concentration and Dr. P. Hobson, who is a native speaker, for revising the manuscript. This work was supported by the Agencia Nacional de Promoción Científica y Técnica (PICT-MICINN 2011 #2772), the Secretaría de Ciencia y Técnica de la Universidad Nacional de Córdoba, the Ministerio de Ciencia y Tecnología de la Provincia de Córdoba (PID 2010), CONICET (PIP # 11220090100109), the Ministerio de Ciencia e Innovación (Grant PRI-PIBAR-2011-1397) and the Ministerio de Economía y Competitividad (Grant SAF 2012-35670). P.P.M.C., A.D.A., P.S.D. and M.G.V. are members of the scientific research career of CONICET. S.V.M.F. and U.G.G. are recipients of PhD fellowships from CONICET. C.A.L. is a recipient of a PhD fellowship from the Agencia Nacional de Promoción Científica y Técnica.

References

[1] S. Palma, R. Manzo, P. Lo Nostro, D. Allemandi, Nanostructures from alkyl vitamin C derivatives (ASCn): properties and potential platform for drug delivery, Int. J. Pharm. 345 (1–2) (2007) 26–34.
[2] S. Palma, R. Manzo, D. Allemandi, L. Fratoni, P. Lo Nostro, Coagels from ascorbic acid derivatives, Langmuir 18 (2002) 9219–9224.
[3] L. Benedini, E.P. Schulz, P. Messina, S. Palma, D. Allemandi, P. Schulz, The ascorbyl palmitate–water system: phase diagram and state of water, Colloids Surf. A Physicochem. Eng. Asp. 375 (2011) 178–185.
[4] S. Palma, R.H. Manzo, D. Allemandi, L. Fratoni, P. Lo Nostro, Solubilization of hydrophobic drugs in octanoyl-6-O-ascorbic acid micellar dispersions, J. Pharm. Sci. 91 (8) (2002) 1810–1816.
[5] S. Palma, R. Manzo, D. Allemandi, L. Fratoni, P. Lo Nostro, Drugs solubilization in ascorbyl-decanoate micellar solutions, Colloids Surf. A Physicochem. Eng. Asp. 212 (2–3) (2003) 163–173.
[6] V. Saino, D. Monti, S. Burgalassi, S. Tampucci, S. Palma, D. Allemandi, P. Chetoni, Optimization of skin permeation and distribution of ibuprofen by using nanostructures (coagels) based on alkyl vitamin C derivatives, Eur. J. Pharm. Biopharm. 76 (3) (2010) 443–449.
[7] M.F. Sanchez Vallecillo, G.V. Ullio Gamboa, S.D. Palma, M.F. Harman, A.L. Chiodetti, G. Moron, D.A. Allemandi, M.C. Pistoresi-Palencia, B.A. Maletto, Adjuvant activity of CpG-ODN formulated as a liquid crystal, Biomaterials 35 (8) (2014) 2529–2542.
[8] S.G. Reed, M.T. Orr, C.B. Fox, Key roles of adjuvants in modern vaccines, Nat. Med. 19 (12) (2013) 1597–1608.
[9] R.L. Coffman, A. Sher, R.A. Seder, Vaccine adjuvants: putting innate immunity to work, Immunity 33 (4) (2010) 492–503.
[10] A.S. McKee, M.K. MacLeod, J.W. Kappler, P. Marrack, Immune mechanisms of protection: can adjuvants rise to the challenge? BMC Biol. 8 (2010) 37.
[11] A.M. Krieg, CpG still rocks! Update on an accidental drug, Nucleic Acid Ther. 22 (2) (2012) 77–89.
[12] F. Steinhagen, T. Kinjo, C. Bode, D.M. Klinman, TLR-based immune adjuvants, Vaccine 29 (17) (2011) 3341–3355.
[13] A.M. Krieg, Therapeutic potential of Toll-like receptor 9 activation, Nat. Rev. Drug Discov. 5 (6) (2006) 471–484.
[14] J. Kovarik, P. Bozzotti, L. Love-Homan, M. Pihlgren, H.L. Davis, P.H. Lambert, A.M. Krieg, C.A. Siegrist, CpG oligodeoxynucleotides can circumvent the Th2 polarization of neonatal responses to vaccines but may fail to fully redirect Th2 responses established by neonatal priming, J. Immunol. 162 (3) (1999) 1611–1617.
[15] D. Alignani, B. Maletto, M. Liscovsky, A. Ropolo, G. Moron, M.C. Pistoresi-Palencia, Orally administered OVA/CpG-ODN induces specific mucosal and systemic immune response in young and aged mice, J. Leukoc. Biol. 77 (6) (2005) 898–905.
[16] B. Maletto, A. Ropolo, V. Moron, M.C. Pistoresi-Palencia, CpG-DNA stimulates cellular and humoral immunity and promotes Th1 differentiation in aged BALB/c mice, J. Leukoc. Biol. 72 (3) (2002) 447–454.
[17] B.A. Maletto, A.S. Ropolo, M.V. Liscovsky, D.O. Alignani, M. Glocker, M.C. Pistoresi-Palencia, CpG oligodeoxinucleotides functions as an effective adjuvant in aged BALB/c mice, Clin. Immunol. 117 (3) (2005) 251–261.
[18] G.K. Mutwiri, A.K. Nichani, S. Babiuk, L.A. Babiuk, Strategies for enhancing the immunostimulatory effects of CpG oligodeoxynucleotides, J. Control. Release 97 (1) (2004) 1–17.
[19] G. Mutwiri, S. van Drunen Littel-van den Hurk, L.A. Babiuk, Approaches to enhancing immune responses stimulated by CpG oligodeoxynucleotides, Adv. Drug Deliv. Rev. 61 (3) (2009) 226–232.
[20] N. Hanagata, Structure-dependent immunostimulatory effect of CpG oligodeoxynucleotides and their delivery system, Int. J. Nanomedicine 7 (2012) 2181–2195.
[21] M. Kool, K. Fierens, B.N. Lambrecht, Alum adjuvant: some of the tricks of the oldest adjuvant, J. Med. Microbiol. 61 (Pt 7) (2012) 927–934.
[22] O. Duramad, K.L. Fearon, B. Chang, J.H. Chan, J. Gregorio, R.L. Coffman, F.J. Barrat, Inhibitors of TLR-9 act on multiple cell subsets in mouse and man in vitro and prevent death in vivo from systemic inflammation, J. Immunol. 174 (9) (2005) 5193–5200.
[23] R.D. Pawar, A. Ramanjaneyulu, O.P. Kulkarni, M. Lech, S. Segerer, H.J. Anders, Inhibition of Toll-like receptor-7 (TLR-7) or TLR-7 plus TLR-9 attenuates glomerulonephritis and lung injury in experimental lupus, J. Am. Soc. Nephrol. 18 (6) (2007) 1721–1731.
[24] S. Rahimian, J.W. Kleinovink, M.F. Fransen, L. Mezzanotte, H. Gold, P. Wisse, H. Overkleeft, M. Amidi, W. Jiskoot, C.W. Lowik, F. Ossendorp, W.E. Hennink, Near-infrared labeled, ovalbumin loaded polymeric nanoparticles based on a hydrophilic polyester as model vaccine: in vivo tracking and evaluation of antigen-specific CD8(+) T cell immune response, Biomaterials 37 (2015) 469–477.

[25] M. Ambrosi, P. Lo Nostro, L. Fratoni, L. Dei, B. Ninham, S. Palma, D. Allemandi, R. Allemandi, P. Baglioni, Water of hydration in coagels, Phys. Chem. Chem. Phys. 1401 (2004).
[26] M. Kool, T. Soullie, M. van Nimwegen, M.A. Willart, F. Muskens, S. Jung, H.C. Hoogsteden, H. Hammad, B.N. Lambrecht, Alum adjuvant boosts adaptive immunity by inducing uric acid and activating inflammatory dendritic cells, J. Exp. Med. 205 (4) (2008) 869–882.
[27] A. Seubert, S. Calabro, L. Santini, B. Galli, A. Genovese, S. Valentini, S. Aprea, A. Colaprico, U. D'Oro, M.M. Giuliani, M. Pallaoro, M. Pizza, D.T. O'Hagan, A. Wack, R. Rappuoli, E. De Gregorio, Adjuvanticity of the oil-in-water emulsion MF59 is independent of Nlrp3 inflammasome but requires the adaptor protein MyD88, Proc. Natl. Acad. Sci. U. S. A. 108 (27) (2011) 11169–11174.
[28] J.T. Norton, T. Hayashi, B. Crain, M. Corr, D.A. Carson, Role of IL-1 receptor-associated kinase-M (IRAK-M) in priming of immune and inflammatory responses by nitrogen bisphosphonates, Proc. Natl. Acad. Sci. U. S. A. 108 (27) (2011) 11163–11168.
[29] N.S. Wilson, B. Yang, A.B. Morelli, S. Koernig, A. Yang, S. Loeser, D. Airey, L. Provan, P. Hass, H. Braley, S. Couto, D. Drane, J. Boyle, G.T. Belz, A. Ashkenazi, E. Maraskovsky, ISCOMATRIX vaccines mediate CD8+ T-cell cross-priming by a MyD88-dependent signaling pathway, Immunol. Cell Biol. 90 (5) (2012) 540–552.
[30] N. Warner, G. Nunez, MyD88: a critical adaptor protein in innate immunity signal transduction, J. Immunol. 190 (1) (2013) 3–4.
[31] J. Scheller, A. Chalaris, D. Schmidt-Arras, S. Rose-John, The pro- and anti-inflammatory properties of the cytokine interleukin-6, Biochim. Biophys. Acta 1813 (5) (2011) 878–888.
[32] O. Soehnlein, L. Lindbom, C. Weber, Mechanisms underlying neutrophil-mediated monocyte recruitment, Blood 114 (21) (2009) 4613–4623.
[33] N.V. Serbina, E.G. Pamer, Monocyte emigration from bone marrow during bacterial infection requires signals mediated by chemokine receptor CCR2, Nat. Immunol. 7 (3) (2006) 311–317.
[34] M. Rasia, M.I. Spengler, S. Palma, R. Manzo, P. Lo Nostro, D. Allemandi, Effect of ascorbic acid based amphiphiles on human erythrocytes membrane, Clin. Hemorheol. Microcirc. 36 (2) (2007) 133–140.
[35] M. Mottola, N. Wilke, L. Benedini, R.G. Oliveira, M.L. Fanani, Ascorbyl palmitate interaction with phospholipid monolayers: electrostatic and rheological preponderancy, Biochim. Biophys. Acta 1828 (11) (2013) 2496–2505.
[36] M. Lamkanfi, V.M. Dixit, Mechanisms and functions of inflammasomes, Cell 157 (5) (2014) 1013–1022.
[37] J. Harris, F.A. Sharp, E.C. Lavelle, The role of inflammasomes in the immunostimulatory effects of particulate vaccine adjuvants, Eur. J. Immunol. 40 (3) (2010) 634–638.
[38] S. Awate, L.A. Babiuk, G. Mutwiri, Mechanisms of action of adjuvants, Front. Immunol. 4 (2013) 114.
[39] R.C. Rowe, P.J. Heskey, S.C. Owen, Handbook of Pharmaceutical Excipients, sixth ed. Pharmaceutical Press, London, 2009. 43–46.
[40] T. Marichal, K. Ohata, D. Bedoret, C. Mesnil, C. Sabatel, K. Kobiyama, P. Lekeux, C. Coban, S. Akira, K.J. Ishii, F. Bureau, C.J. Desmet, DNA released from dying host cells mediates aluminum adjuvant activity, Nat. Med. 17 (8) (2011) 996–1002.
[41] A.S. McKee, M.A. Burchill, M.W. Munks, L. Jin, J.W. Kappler, R.S. Friedman, J. Jacobelli, P. Marrack, Host DNA released in response to aluminum adjuvant enhances MHC class II-mediated antigen presentation and prolongs CD4 T-cell interactions with dendritic cells, Proc. Natl. Acad. Sci. U. S. A. 110 (12) (2013) E1122–E1131.
[42] M. Vono, M. Taccone, P. Caccin, M. Gallotta, G. Donvito, S. Falzoni, E. Palmieri, M. Pallaoro, R. Rappuoli, F. Di Virgilio, E. De Gregorio, C. Montecucco, A. Seubert, The adjuvant MF59 induces ATP release from muscle that potentiates response to vaccination, Proc. Natl. Acad. Sci. U. S. A. 110 (52) (2013) 21095–21100.
[43] K. Eguchi, I. Manabe, Y. Oishi-Tanaka, M. Ohsugi, N. Kono, F. Ogata, N. Yagi, U. Ohto, M. Kimoto, K. Miyake, K. Tobe, H. Arai, T. Kadowaki, R. Nagai, Saturated fatty acid and TLR signaling link beta cell dysfunction and islet inflammation, Cell Metab. 15 (4) (2012) 518–533.
[44] R.G. Snodgrass, S. Huang, I.W. Choi, J.C. Rutledge, D.H. Hwang, Inflammasome-mediated secretion of IL-1beta in human monocytes through TLR2 activation; modulation by dietary fatty acids, J. Immunol. 191 (8) (2013) 4337–4347.
[45] M. Zaman, I. Toth, Immunostimulation by synthetic lipopeptide-based vaccine candidates: structure–activity relationships, Front. Immunol. 4 (2013) 318.
[46] T.L. Flach, G. Ng, A. Hari, M.D. Desrosiers, P. Zhang, S.M. Ward, M.E. Seamone, A. Vilaysane, A.D. Mucsi, Y. Fong, E. Prenner, C.C. Ling, J. Tschopp, D.A. Muruve, M.W. Amrein, Y. Shi, Alum interaction with dendritic cell membrane lipids is essential for its adjuvanticity, Nat. Med. 17 (4) (2011) 479–487.
[47] T.A. Barr, S. Brown, P. Mastroeni, D. Gray, B cell intrinsic MyD88 signals drive IFN-gamma production from T cells and control switching to IgG2c, J. Immunol. 183 (2) (2009) 1005–1012.
[48] M. Schnare, G.M. Barton, A.C. Holt, K. Takeda, S. Akira, R. Medzhitov, Toll-like receptors control activation of adaptive immune responses, Nat. Immunol. 2 (10) (2001) 947–950.
[49] R. Lande, J. Gregorio, V. Facchinetti, B. Chatterjee, Y.H. Wang, B. Homey, W. Cao, B. Su, F.O. Nestle, T. Zal, I. Mellman, J.M. Schroder, Y.J. Liu, M. Gilliet, Plasmacytoid dendritic cells sense self-DNA coupled with antimicrobial peptide, Nature 449 (7162) (2007) 564–569.
[50] A.B. Imaeda, A. Watanabe, M.A. Sohail, S. Mahmood, M. Mohamadnejad, F.S. Sutterwala, R.A. Flavell, W.Z. Mehal, Acetaminophen-induced hepatotoxicity in mice is dependent on Tlr9 and the Nalp3 inflammasome, J. Clin. Invest. 119 (2) (2009) 305–314.
[51] S.R. Paludan, A.G. Bowie, Immune sensing of DNA, Immunity 38 (5) (2013) 870–880.
[52] C.A. Dinarello, Immunological and inflammatory functions of the interleukin-1 family, Annu. Rev. Immunol. 27 (2009) 519–550.
[53] S.A. Nish, D. Schenten, F.T. Wunderlich, S.D. Pope, Y. Gao, N. Hoshi, S. Yu, X. Yan, H.K. Lee, L. Pasman, I. Brodsky, B. Yordy, H. Zhao, J. Bruning, R. Medzhitov, T cell-intrinsic role of IL-6 signaling in primary and memory responses, Elife 3 (2014) e01949.
[54] G. Hui, C. Hashimoto, Interleukin-6 has differential influence on the ability of adjuvant formulations to potentiate antibody responses to a *Plasmodium falciparum* blood-stage vaccine, Vaccine 25 (36) (2007) 6598–6603.